

Doping Dependence of the Second Magnetization Peak, Critical Current Density and Pinning Mechanism in $\text{BaFe}_{2-x}\text{Ni}_x\text{As}_2$ Pnictide Superconductors

Shyam Sundar^{*,†}, Said Salem-Sugui Jr.[†], Edmund Lovell[‡], Alexander Vanstone[‡], Lesley F
Cohen[‡], Dongliang Gong[¶], Rui Zhang[§], Xingye Lu^{II}, Huiqian Luo[¶], Luis Ghivelder[†].

[†]*Instituto de Física, Universidade Federal do Rio de Janeiro,
21941-972 Rio de Janeiro, RJ, Brazil*

[‡]*The Blackett Laboratory, Physics Department,
Imperial College London, London SW7 2AZ, United Kingdom*

[¶]*Beijing National Laboratory for Condensed Matter Physics,
Institute of Physics, Chinese Academy of Sciences,
Beijing 100190, People's Republic of China*

[§]*Department of Physics and Astronomy,
Rice University, Houston, Texas 77005, USA and*

^{II}*Center for Advanced Quantum Studies and Department of Physics,
Beijing Normal University, Beijing 100875, China**

Abstract

A series of high quality $\text{BaFe}_{2-x}\text{Ni}_x\text{As}_2$ pnictide superconductors were studied using magnetic relaxation and isothermal magnetic measurements in order to study the second magnetization peak (SMP) and critical current behaviour in Ni-doped 122 family. The temperature dependence of the magnetic relaxation rate suggests a pinning crossover, whereas, its magnetic field dependence hints a vortex-lattice structural phase-transition. The activation energy (U) estimated using the magnetic relaxation data was analyzed in detail for slightly-underdoped, slightly-overdoped and an overdoped samples, using Maley's method and collective creep theory. Our results confirm that the SMP in these samples is due to the collective (elastic) to plastic creep crossover as has been observed for the other members of 122-family. In addition, we also investigated the doping dependence of the critical current density (J_c) and the vortex-pinning behaviour in these compounds. The observed J_c is higher than the threshold limit (10^5 A/cm^2) considered for the technological potential and even greater than 1 MA/cm^2 for slightly underdoped Ni-content, $x = 0.092$ sample. The pinning characteristics were analyzed in terms of the models developed by Dew-Hughes and Griessen *et al*, which suggest the dominant role of δl -type pinning.

* shyam.phy@gmail.com

I. INTRODUCTION

The study of vortex dynamics in type-II superconductors gained the interest of experimentalists and theoreticians as soon as the creep phenomenon in magnetization was observed in conventional low T_c systems [1–3]. From a technological point of view, the creep behaviour in magnetization is directly related to a creep in the critical current showing the importance to understand the vortex pinning mechanism. Later, the study of vortex dynamics gained attention in the late 80s with the discovery of the high- T_c cuprates, which shows an intrinsic giant thermal activated magnetic relaxation [4] as well as the so called second magnetization peak (SMP) effect in the isothermal magnetization curves which renders a peak in the critical currents [5–8], as also observed in the low T_c superconductors, such as, Nb [9]. More recently (2008), the study of vortex dynamics regained the attention of the scientific community due to the discovery of the iron-pnictide and iron selenide superconductors [10–13] with a moderately high- T_c (from 20 K up to 56 K) [14], large upper critical fields, H_{c2} [15, 16], small anisotropy [17–19] and better intergrain connectivity than the cuprates [20, 21]. These salient features of iron pnictide superconductors are potentially suitable for applications purposes [22]. Besides, pnictides are known as multiband superconductors, which may play a role on the pinning of vortices through the inter-band and intra-band electron scatterings [23]. Since then, vortex dynamics studies were performed on different pnictides compounds discovered over the years [13, 24–31], and, most of them are devoted to the study of the mechanism responsible for the appearance of SMP in isothermal magnetization curves. Contrary to the cuprates, where the SMP is mostly observed only for $H \parallel$ c-axis, in Fe-pnictides, due to the low anisotropy, it is observed for both, $H \parallel$ c-axis and $H \parallel$ ab planes. A rich variety of mechanisms were proposed as responsible for the SMP in different iron-pnictide superconductors, such as, crossover from elastic to plastic [30, 32, 33], order-disorder transition [27, 34] and vortex-lattice phase transitions [25, 35]. However, the mechanism responsible for SMP in Ni-doped BaFe_2As_2 pnictide superconductors is as yet unresolved [29, 36, 37]. Interestingly, in iron-pnictide superconductors, it has been observed that the existence of the SMP is doping dependent [31, 38].

This motivated us to investigate the vortex-dynamics in a series of high quality $\text{BaFe}_{2-x}\text{Ni}_x\text{As}_2$ ($x = 0.092, 0.108, 0.12, 0.15, 0.18, 0.065$) pnictide superconductors. In addition to the detailed study of the SMP in different Ni-content samples, a complementary study of the

critical current density and the pinning behaviour is also performed on all samples using magnetic relaxation and isothermal magnetic measurements. A detailed analysis of the magnetic relaxation data using Maley's method [39] and collective pinning theory [40] unambiguously shows that the SMP in Ni-doped BaFe_2As_2 compounds is due to the collective (elastic) to plastic creep crossover, which might be accompanied by a vortex-lattice structural phase transition, similar to the Co-doped BaFe_2As_2 superconductor. The critical current density is found to be higher than the threshold limit ($> 10^5 \text{ A/cm}^2$) considered for technological applications. The doping dependence of critical current density, $J_c(x)$, does not follow the variation of superconducting transition temperature with Ni-content, $T_c(x)$, and shows a spike-feature at $x = 0.092$. The dominant pinning in these crystals is found to be related to the variation of the charge carrier mean free path, generally known as δl -type pinning.

II. EXPERIMENTAL DETAILS

A detailed study on a series of six $\text{BaFe}_{2-x}\text{Ni}_x\text{As}_2$ pnictide superconductors is performed. Details of the crystal growth are described in Ref. [41]. Large crystals were cut into small pieces with typical dimensions of $2.5 \text{ mm} \times 1 \text{ mm} \times 0.15 \text{ mm}$, using a clean scalpel and the samples with sharpest superconducting transition were chosen for each concentration to study. Surface maps of T_c , measured for two chosen samples ($x = 0.092, 0.108$) using a scanning Hall probe magnetometer with a $5 \mu\text{m} \times \mu\text{m}$ active area of the Hall sensor ($1 \mu\text{m}$ thick InSb epilayer on undoped GaAs substrate) [42] are shown in Fig. 1. A 4 T split coil superconducting magnet and a continuous flow helium cryostat (Oxford Instruments Ltd.) were used to perform the measurements. The imaging was performed by applying 1 mT magnetic field (parallel to the c-axis) in zero field cooled state below T_c , and mapping the Meissner current profile across the crystal. At low temperature the screen current perfectly follows the edge of the sample. The mapping shows that the T_c distribution within the crystals studied, are rather uniform and of high quality. The screening diminishes from the edges towards the center of the sample as expected within the measured transition width, consistent with the global magnetometry $M(T)$ data. Magnetization measurements were performed using a vibrating sample magnetometer (VSM, Quantum Design, USA), where the sample was mounted between the two quartz cylinders in a brass sample holder. The

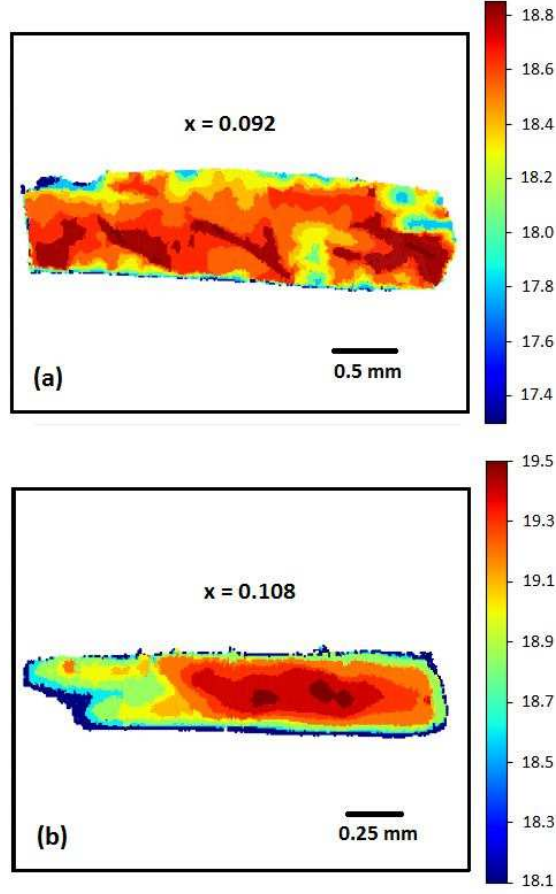


FIG. 1. Distribution of the superconducting transition temperature (T_c) in (a) $x = 0.092$ and (b) $x = 0.108$ samples, measured using a scanning Hall probe magnetometer. Variation of the T_c over the scanned surface is identified by labels in each panel. Both images show the good quality of the samples.

temperature and magnetic field dependence of the magnetization, $M(T)$, $M(H)$, and the magnetic relaxations, $M(t)$, were measured for $H \parallel c$ -axis down to 2K and up to 9T magnetic field, in zero field cooled (zfc) mode. To investigate the behaviour of SMP in the samples, each $M(t)$ was measured over a period of approximately 90 minutes at fixed magnetic field in the increasing cycle of the isothermal, $M(H)$ curves.

III. RESULTS AND DISCUSSION

Figure 2 shows the temperature dependence of magnetization, $M(T)$, measured for all samples in zfc mode with $H = 1$ mT. The sharp drop in the magnetization for diamagnetic

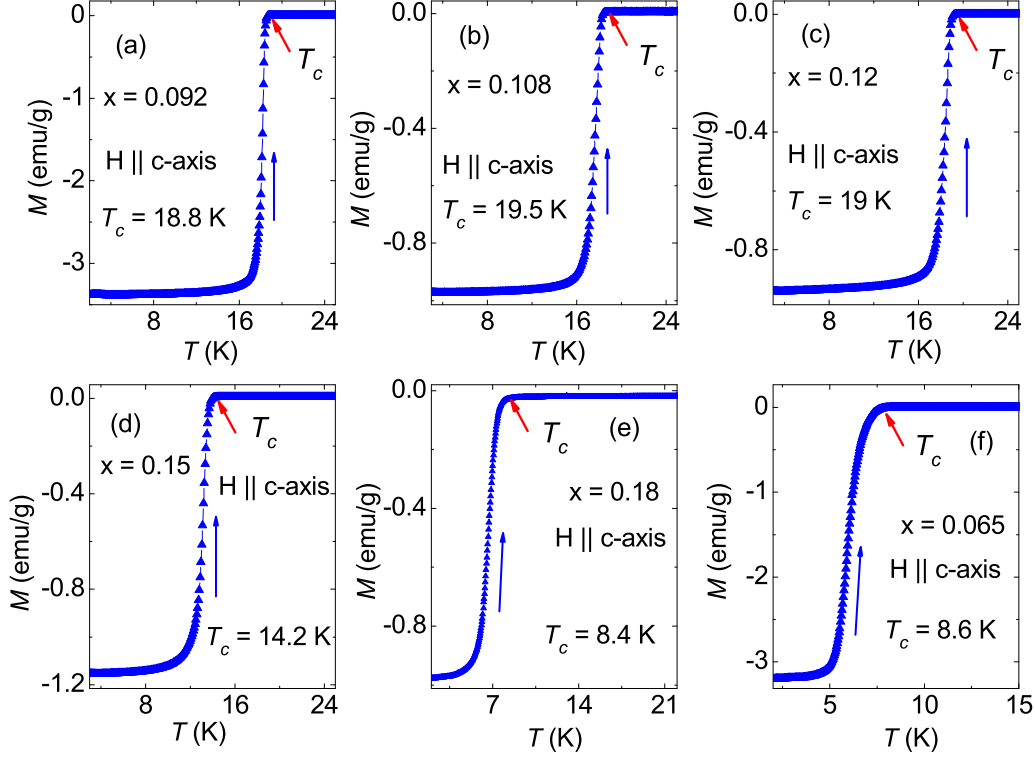


FIG. 2. (a-f) Temperature dependence of magnetization, $M(T)$, of $\text{BaFe}_{2-x}\text{Ni}_x\text{As}_2$ pnictide superconductors measured in zfc mode with $H = 1$ mT.

signal is considered as the onset of the superconducting transition (T_c), shown with an arrow in Fig. 2. The sharp superconducting transition is an indication of the good quality of the samples and the obtained T_c values are in fair agreement with the available literature [41, 43]. For $\text{BaFe}_{2-x}\text{Ni}_x\text{As}_2$ superconductors, the optimal doping is $x = 0.1$, with $T_c = 20.1$ K [41, 43]. In the present study, the maximum $T_c = 19.5$ K, is observed for $x = 0.108$, which is slightly overdoped and for more overdoped samples T_c decreases. Similarly, $x = 0.092$ is slightly underdoped and shows the $T_c = 18.8$ K, which further decreases for more underdoped samples.

A. Magnetic relaxation and the second magnetization peak (SMP)

Figure 3 shows selected isothermal $M(H)$ curves, measured in zfc mode at various temperatures below T_c down to 2 K. The symmetric behaviour of isothermal $M(H)$ suggests the dominant role of bulk pinning for all samples under study. A clear signature of the SMP is observed for each doping content, except for the highly underdoped, $x = 0.065$ sample.

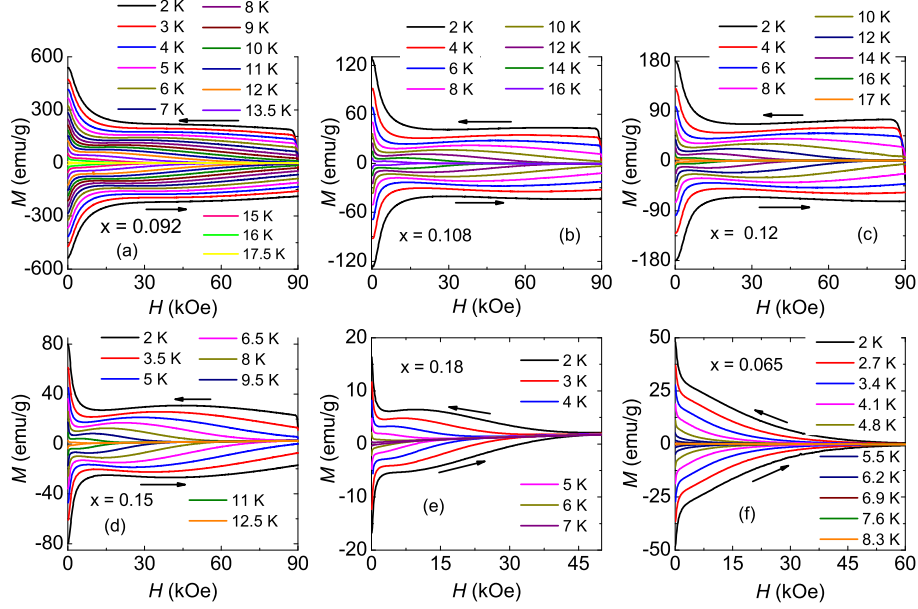


FIG. 3. Isothermal magnetic field dependence of magnetization, $M(H)$, for $x =$ (a) 0.092, (b) 0.108, (c) 0.12, (d) 0.15, (e) 0.18, and (f) 0.065 $\text{BaFe}_{2-x}\text{Ni}_x\text{As}_2$ pnictide superconductors, in field increasing and field decreasing cycle. Each sample show the second magnetization peak feature below T_c , except the highly underdoped, $x = 0.065$ sample.

The absence of SMP in $x = 0.065$ sample is might be due to the static antiferromagnetic long-range order, which exists in low doped $\text{BaFe}_{2-x}\text{Ni}_x\text{As}_2$ samples [44]. The onset and the peak position of the SMP are defined as H_{on} and H_P respectively. The magnetic hysteresis in the field increasing and field decreasing cycles of the $M(H)$ vanishes at higher fields, defined as the irreversibility field, H_{irr} . Interestingly, in slightly underdoped composition, $x = 0.092$, the SMP is smeared out below 5 K. This is called faded SMP, as seen in Fig. 4 (a). To confirm this anomaly, we repeated the measurements on another crystal with same x content (same T_c) and observed the same behaviour. Similar anomalous behaviour has also been observed in Bi-Sr-Ca-Cu-O single crystal, where, the SMP was only observed in a temperature range of 20-40 K below T_c [45, 46]. In contrast to that, a recent study on $\text{Ba}_{0.75}\text{K}_{0.25}\text{Fe}_2\text{As}_2$ superconductor showed the SMP only at temperatures below $T_c/2$ and vanished at higher temperatures [30].

To investigate the origin of the SMP in $\text{BaFe}_{2-x}\text{Ni}_x\text{As}_2$, with $x = 0.092$ (slightly underdoped), $x = 0.108$ (slightly overdoped), $x = 0.15$ (overdoped) superconductors, we performed magnetic relaxation, $M(t)$ at selected temperature and magnetic field values for ~ 90 min-

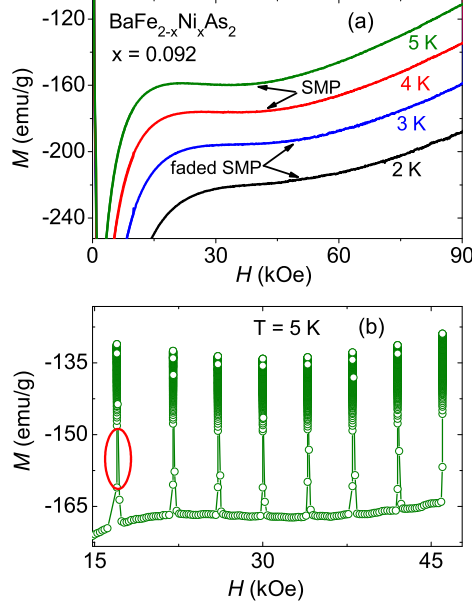


FIG. 4. (a) Isothermal $M(H)$ for $\text{BaFe}_{2-x}\text{Ni}_x\text{As}_2$, $x = 0.092$ sample at some selected temperatures, where, below $T = 4$ K, the SMP feature smeared out. (b) Isothermal $M(H)$ at $T = 5$ K with magnetic relaxation data measured for selected magnetic fields. The circle highlights the rapid magnetic relaxations for first 15 seconds.

utes in the lower branch of the $M(H)$ curves. In Fig. 4 (b), magnetic relaxation results are shown for $x = 0.092$ at $T = 5$ K. A circle in Fig. 4 (b) highlights the initial 15 seconds of relaxation, which corresponds to ~ 40 % of the total magnetic relaxation in a period of 90 minutes of measurement. This feature is observed in all samples under investigation and is also found in a recent study on $\text{Ba}_{0.75}\text{K}_{0.25}\text{Fe}_2\text{As}_2$ [30]. All magnetic relaxations follow the usual logarithmic behaviour with time, $|M| \sim \log(t)$ and the plots of $\ln|M|$ vs $\ln t$ allowed us to obtain the relaxation rate, $R = d\ln|M|/d\ln t$.

Figure 5 shows the relaxation rate as a function of magnetic field for samples with $x = 0.092, 0.108, 0.15$ and 0.065 . For each Ni content, a peak in $R(H)$ associated to the SMP is observed in each curve. A similar feature has also been observed in the SMP study of Co-doped BaFe_2As_2 and explained in terms of the vortex-lattice structural phase transition [25, 32]. It is worth mentioning the absence of peak in $R(H)$ for $x = 0.065$ sample, which do not show the SMP.

The characteristic magnetic fields associated with the SMP, H_{on} and H_p , H_{irr} , and H_m are shown in Fig. 6 with H_{on} and H_p lying far below the H_{irr} line. It should be noted that

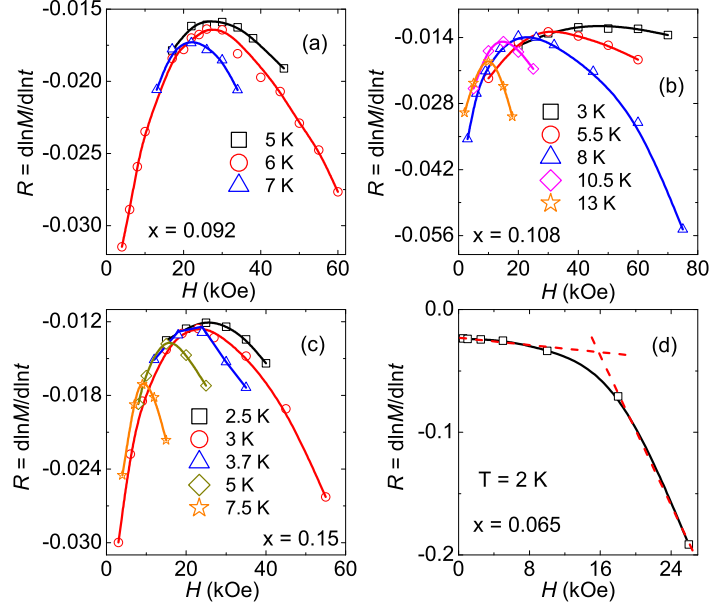


FIG. 5. Magnetic field dependence of relaxation rate, $R = d\ln|M|/d\ln t$, for $\text{BaFe}_{2-x}\text{Ni}_x\text{As}_2$, $x =$ (a) 0.092, (b) 0.108, (c) 0.15 and (d) 0.065 samples. Each sample shows the clear peak structure in every isothermal $R(H)$, except $x = 0.065$ sample, which also does not show the second magnetization peak feature.

the behaviour of the temperature dependence of H_p is different in $x = 0.092$, compared to the other samples used in this study. It should also be noted that H_m lies in between the H_{on} and H_p lines as previously observed in the case of Co-doped BaFe_2As_2 [25, 32]. Since, the peak position, H_m , in H - T phase diagram varies with temperature in a similar way as observed for $\text{Ba}(\text{Fe}_{0.925}\text{Co}_{0.075})_2\text{As}_2$ [25], we suggest that this behaviour might be associated with the vortex-lattice structural phase transition in the present study. However, it is argued that such vortex-lattice structural phase transition may be followed by a crossover in creep behaviour [6, 25, 32].

Figure 7, shows the temperature dependence of the relaxation rate, $R(T)$, for $x = 0.108$ and 0.15 measured with different magnetic fields. Each isofield $R(T)$, for both samples, shows a clear change of slope at T_{cr} . Interestingly, T_{cr} values obtained from Fig. 7 (a)-(d) are well matched with the H_p line in the H - T phase-diagram suggesting that a pinning crossover is responsible for the SMP. A peak behaviour observed simultaneously in isofield $R(T)$ and $R(H)$ has been argued as a possibility for a vortex-lattice structural phase-transition in different superconductors [25, 35, 47], but in the present case the peak positions of $R(H)$

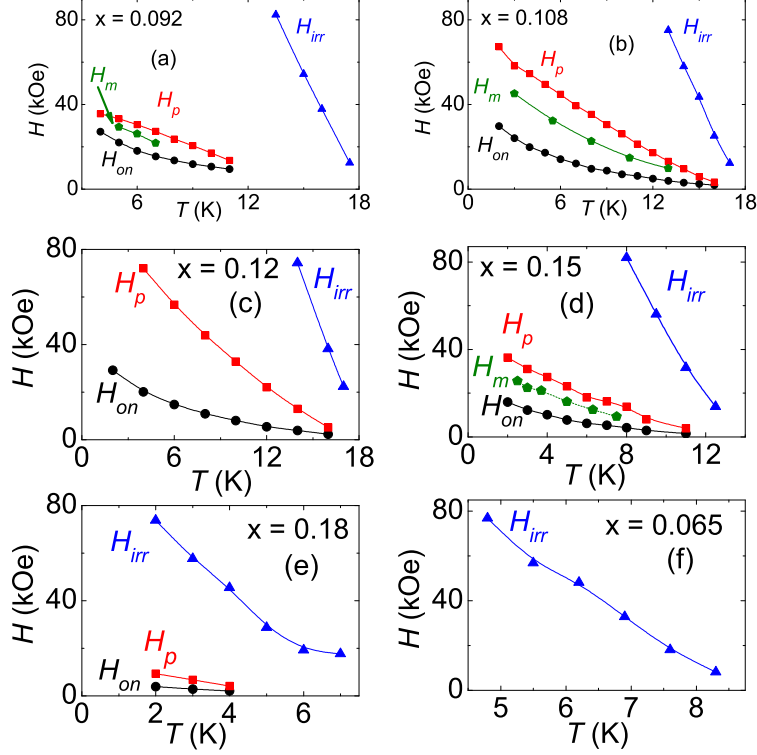


FIG. 6. The H - T phase-diagram for $x =$ (a) 0.092, (b) 0.108, (c) 0.12, (d) 0.15, (e) 0.18, and (f) 0.065 samples. The characteristic fields, H_{on} , H_p , H_{irr} , and H_m are well explained in the text.

and $R(T)$ do not match. As we see in Fig. 5, each isothermal $R(H)$ shows a peak behaviour, however, the isofield $R(T)$ shown in Fig. 7 (a-d), only show a change of slope and do not exhibit a clear peak structure.

We exploited the temperature dependence of the relaxation rate, $R(T)$, to obtain the activation energy ($U^* = T/R$), and plotted it in Fig. 8 as a function of the inverse current density, $1/J$, where J is obtained using the Bean's critical state model, as discussed later. A U^* vs. $1/J$ plot has been extensively used to investigate the vortex dynamics in pnictide superconductors [30, 32, 33, 48]. To relate the activation energy (U^*) with the critical current density (J_c), we used an expression from the theory of collective flux creep [40], $U^* = U_0(J_c/J)^\mu$, where, μ and J_c depend on the dimensionality and size of the flux bundles under consideration [40]. Using this expression, the exponent μ may be obtained by double logarithmic plot of U^* vs. $1/J_c$, which is shown in Fig. 8 (a) and (b) for $x = 0.108$ and 0.15 samples respectively. For a 3-dimensional system, the predicted values of exponent μ are reported as $1/7$, $3/2$ and $7/9$, for single-vortex, small-bundle, and large-bundle regimes,

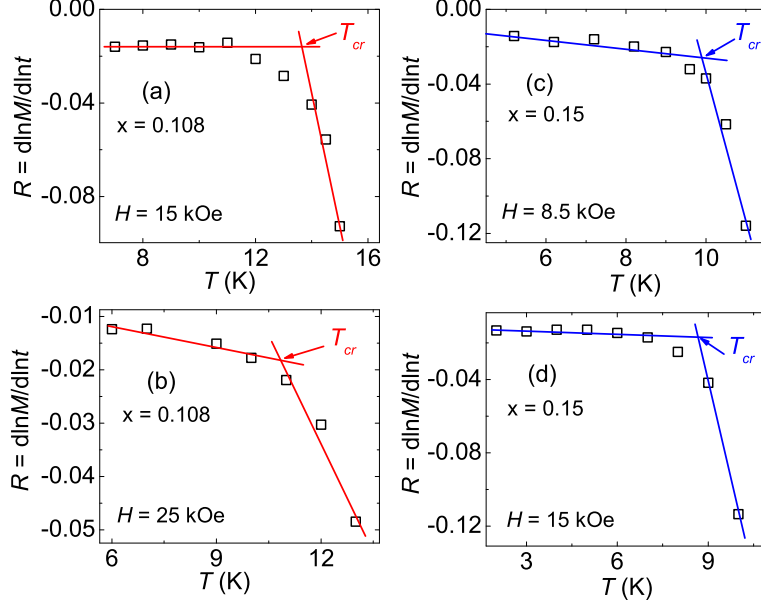


FIG. 7. Temperature dependence of relaxation rate, $R = d\ln|M|/d\ln T$, for $\text{BaFe}_{2-x}\text{Ni}_x\text{As}_2$, $x =$ (a, b) 0.108 and (c, d) 0.15 samples. Each isofield $R(T)$ shows a crossover in slope, which is defined as T_{cr} . The crossover in the slope suggests the crossover in pinning behaviour and is apparently related to the second magnetization peak (H_p) in the sample.

respectively [40, 49]. However, the obtained μ values for $x = 0.108$ are 1.1 and 0.59 for $H=15$ and 25 kOe and μ for $x=0.15$ are 0.8 and 2.7 for $H = 8.5$ and 15 kOe respectively (see Fig. 8 (a), (b)). These μ values are different than the predicted ones, as found in other studies on several superconductors [24, 27, 33, 50–52]. Similarly, values of the exponent (p) at higher temperature side (low J) is also found to be different than the predicted value for plastic creep ($p = 0.5$) [5, 32]. Although, the observed exponents in Fig. 8 (a,b) are different than the expected values, the plots of U^* vs. $1/J$ in the present study suggest a crossover in the pinning mechanism is responsible for SMP.

In order to confirm a possible pinning crossover, observed in Fig. 7 and Fig. 8 for $R(T)$ and $U^*(1/J)$ curves respectively, we plotted the activation energy, U , of the, $x = 0.092$, and 0.15, samples, as a function of magnetization, M , by invoking the method developed by Maley *et al* [39] (Similar results are observed for $x = 0.108$, but not shown here). Such methodology has been widely used to investigate the vortex dynamics associated with SMP in different iron pnictide superconductors [30, 31, 33, 38, 39, 50], and is expressed below.

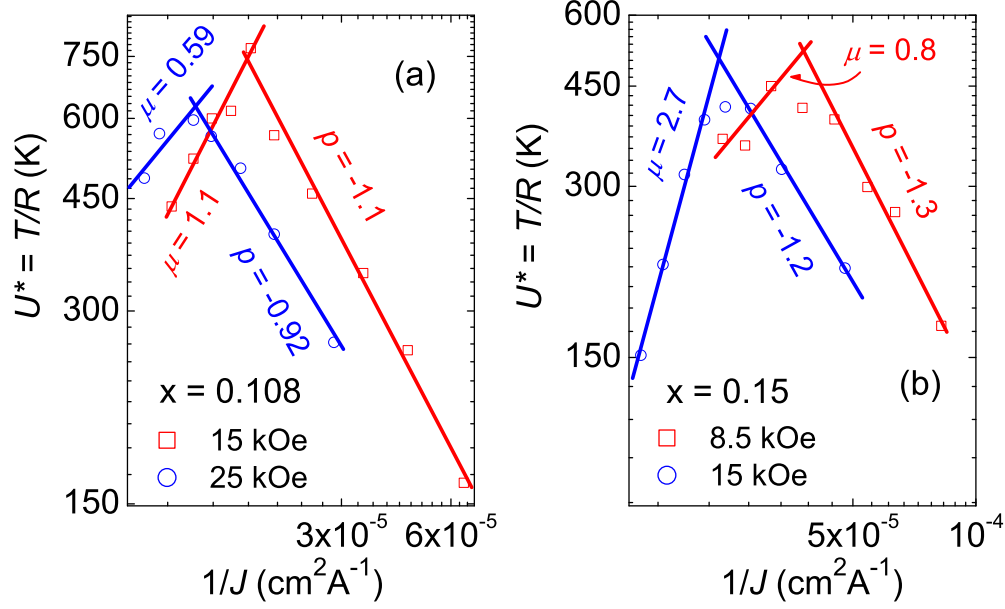


FIG. 8. Activation energy ($U^* = T/R$) as a function of the inverse current density ($1/J$) for $\text{BaFe}_{2-x}\text{Ni}_x\text{As}_2$, $x =$ (a) 0.108 and (b) 0.15 samples. For both samples, value of the parameters (μ and p) in each curve suggests the elastic to plastic pinning crossover and the crossover point is well matched with the H_p .

$$U = -T \ln[dM(t)/dt] + CT, \quad (1)$$

where C is a constant which depends on the hoping distance of the vortex, the attempt frequency and the sample size. The activation energy as a function of magnetization is plotted in Fig. 9 (a, b) for $x = 0.092$ and $x = 0.15$ samples respectively. The insets in Figs. 9 (a, b) show the U vs. M curves for $x = 0.092$, and 0.15 samples using $C = 16$, 25 , 15 respectively. Similar values have been previously reported [32, 50, 53]. The U vs. M curves for each sample, as shown in the insets figures, do not show a smooth behaviour. The curves showing a smooth power law behaviour are obtained after divided U by $g(T/T_c) = (1 - T/T_c)^{1.5}$, as suggested in Ref. [53] and verified in numerous studies [30–32, 38, 50]. The smooth curves of $U/(1 - T/T_c)^{1.5}$ vs. M are shown in each main panel of Fig. 9. The values of the parameter C used in Fig. 9 are employed to extract the activation energy from the magnetic relaxation data in different field regimes, such as, $H < H_{on}$, $H_{on} < H < H_p$ and $H > H_p$, in order to investigate the SMP behaviour in $x = 0.092$, 0.108 and $x = 0.15$ samples (Results for $x = 0.108$ are not shown here).

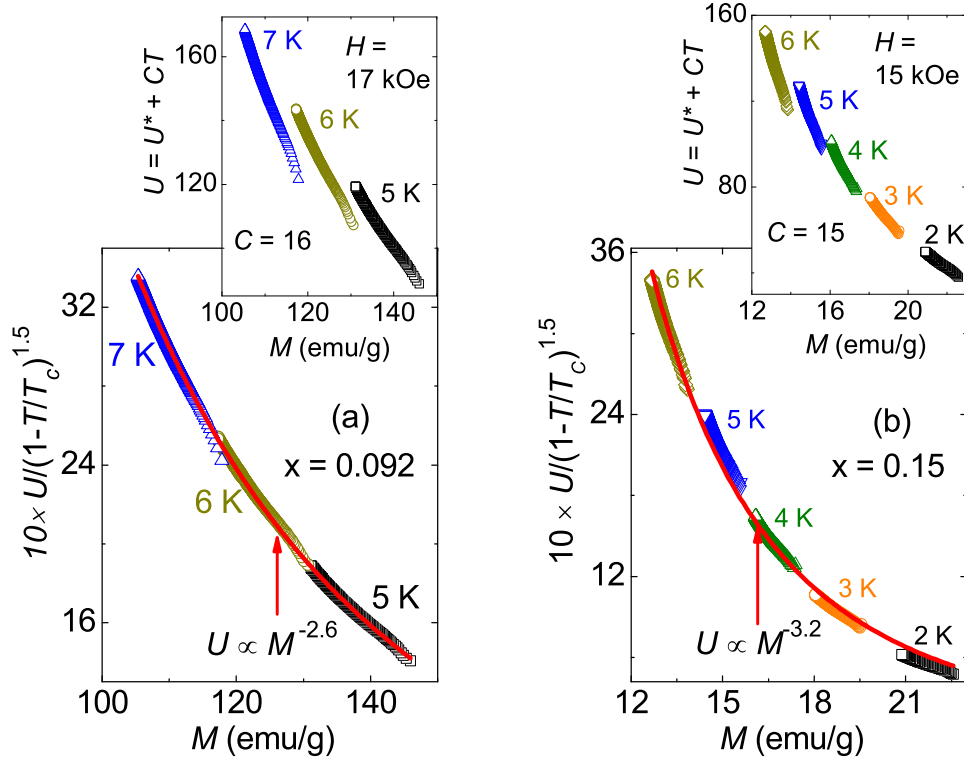


FIG. 9. Variation of activation energy (U) scaled with a function, $g(T/T_c) = (1-T/T_c)^{1.5}$, is plotted as a function of magnetization (M), for $\text{BaFe}_{2-x}\text{Ni}_x\text{As}_2$, $x =$ (a) 0.092, and (b) 0.15 samples. Each scaled curve follow the power law behaviour. Inset of each panel shows $U(M)$ before scaling by $g(T/T_c)$ function. Similar results are also observed for $x = 0.108$ sample (not shown here).

To demonstrate the origin of the SMP in a series of $\text{BaFe}_{2-x}\text{Ni}_x\text{As}_2$, we plotted the activation energy as a function of magnetization, $U(M)$, shown in the inset of each panel of Fig. 10. For $x = 0.092$, and 0.15 samples, the $U(M)$ curves were plotted for $T = 6$ K, and 3 K respectively in three different magnetic field regimes. These $U(M)$ curves were analyzed in terms of the theory of collective flux creep [5, 40], in which, the activation energy is defined as-

$$U(B, J) = B^\nu J^{-\mu} \approx H^\nu M^{-\mu}, \quad (2)$$

where, the exponents ν and μ depend on the specific pinning regime. According to the collective creep theory, the activation energy (U) increases with the magnetic field (H) and if the activation energy decreases with increasing magnetic field, it is suggestive of plastic creep behaviour [5]. Therefore, in equation 2, the positive value of ν suggests a collective

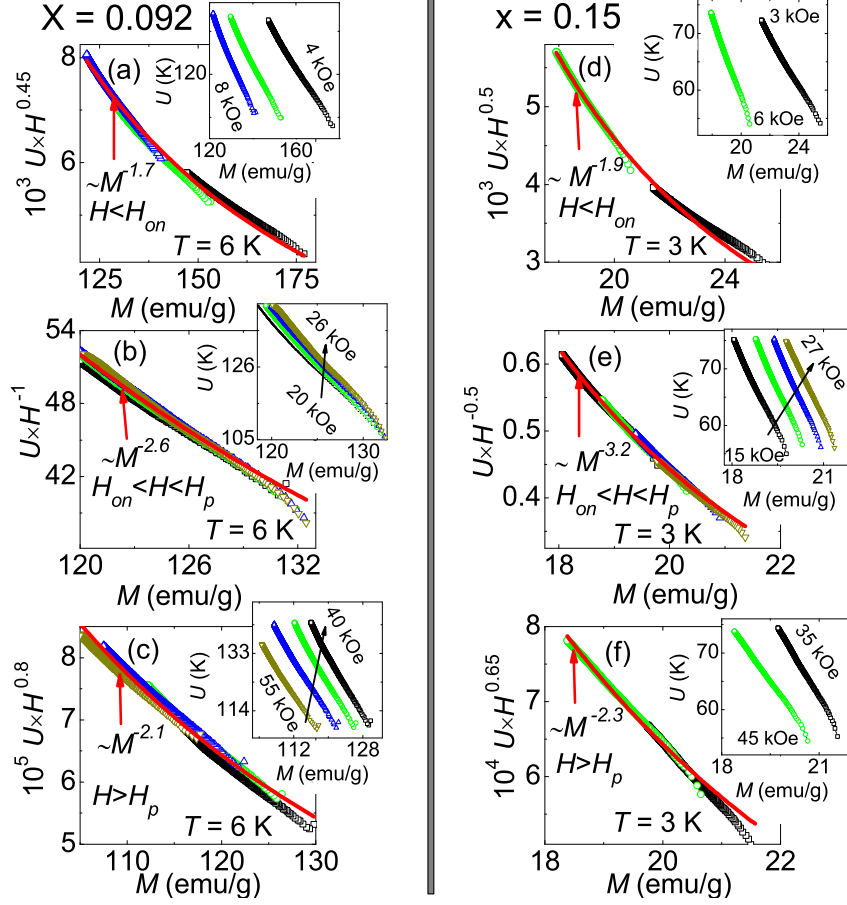


FIG. 10. Activation energy (U) scaled using the theory of collective flux creep is plotted as a function of magnetization (M) in panles, (a)-(c) for $x = 0.092$ and panels (d)-(f) for $x = 0.15$, in different magnetic field regimes (see text). Each sample shows the collective (elastic) to plastic creep crossover. Each inset shows the U vs. M without scaling in different magnetic field regimes. Similar results are also observed for $x = 0.108$ sample (not shown here).

creep mechanism and similarly, a negative value indicates plastic creep [5, 40]. In order to examine the collective (elastic) to plastic creep crossover in the samples, we scaled U with H^ν for each sample under investigation in different magnetic field regimes for different values of ν , as shown in Fig. 10. The positive and negative values of the exponent ν in $H_{on} < H < H_p$ and $H > H_p$ magnetic field regions for each sample ($x = 0.092$ and 0.15), clearly demonstrate the collective (elastic) to plastic creep crossover as the origin of SMP in $\text{BaFe}_{2-x}\text{Ni}_x\text{As}_2$. Similar, elastic to plastic creep crossover is also observed for $x = 0.108$ sample, as the origin for SMP, but results are not shown here. In Figs. 10 (a), and 10 (d), the scaling of U vs. M curves for $H < H_{on}$ also shows the negative value of ν which would

indicate the unphysical plastic creep nature. However, such behaviour is observed in other studies and has been well explained in terms of single vortex pinning (SVP) [5, 30, 32, 33, 50]. The crossover from SVP to collective creep renders a peak at H_{on} , which is entirely different in nature than the SMP at H_p .

B. Critical current density and pinning behaviour

The magnetic field dependence of critical current density, $J_c(x)$, at $T = 2$ K, for each Ni content is shown in Fig. 11 (a). Bean's critical state model [54] is exploited to extract the J_c , using, J_c (A cm^{-2}) = $20\Delta M/a(1 - a/3b)$, where, ΔM (emu cm^{-3}) is the difference between the upper and lower branches of the isothermal $M(H)$ curves and a , b are the dimensions of a rectangular shaped sample ($a < b$ in cm) perpendicular to the applied magnetic field direction [32, 55]. The critical current density (J_c) in iron-based superconductors is quite important for their potential use in technological applications [55, 56]. The maximum, $J_c \approx 2 \text{ MA/cm}^2$, is observed for the slightly underdoped sample, $x = 0.092$, in the zero field limit at $T = 2$ K. On the other hand, for overdoped compounds ($x = 0.108, 0.12, 0.15$), J_c is found to be higher than the threshold limit for technological application ($\approx 10^5 \text{ A/cm}^2$) in the zero magnetic field limit, even at liquid helium temperature ($T = 4.2$ K). For further Ni doping, $x = 0.18$, J_c decreases to the 10^4 A/cm^2 order of magnitude. It is found that the J_c corresponding to the optimal doping ($x = 0.1$) [26, 57] is smaller than the slightly underdoped ($x = 0.9$) regime [58], as has been also observed in the case of $\text{Ba}_{1-x}\text{K}_x\text{Fe}_2\text{As}_2$ [55]. The J_c values above 10^5 A/cm^2 in overdoped samples and even more than 1 MA/cm^2 in slightly underdoped compound makes $\text{BaFe}_{2-x}\text{Ni}_x\text{As}_2$ a potential candidate for application purpose [56].

Figure 11 (b) shows the behavior of J_c as a function of Ni content (x) measured at $T = 2$ K for different magnetic field values. It is interesting to see that $J_c(x)$ shows a spike like behaviour at $x = 0.092$ for each curve plotted for $H = 10 \text{ kOe}, 50 \text{ kOe}, 80 \text{ kOe}$. Interestingly, the $J_c(x)$ curve shown in Fig. 11 (b) is distinctively different than the $T_c(x)$ plot presented in Fig. 11 (c) which shows a broad dome like behaviour [17, 41] instead the spike like peak shown in Fig. 11. Such behaviour between $J_c(x)$ and $T_c(x)$ was also seen by Song *et al*, in $\text{Ba}_{1-x}\text{K}_x\text{Fe}_2\text{As}_2$ [55].

To investigate the pinning behaviour in $\text{BaFe}_{2-x}\text{Ni}_x\text{As}_2$, we estimate the pinning force

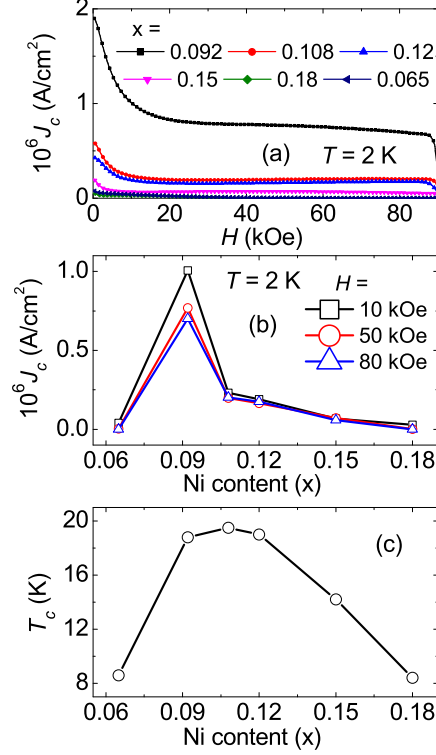


FIG. 11. (a) Comparison of the magnetic field dependence of the critical current density, $J_c(H)$, at $T = 2$ K, between distinct doping (x) contents in $\text{BaFe}_{2-x}\text{Ni}_x\text{As}_2$ superconductors. (b) Critical current density at $T = 2$ K plotted as a function of Ni content (x). The maximum in $J_c(x)$ corresponds to $x = 0.092$. (c) Doping dependence (x) of the superconducting transition temperature (T_c). Peak in $T_c(x)$ corresponds to the $x = 0.108$, however, the optimal doping for $\text{BaFe}_{2-x}\text{Ni}_x\text{As}_2$ superconductors is $x = 0.1$ [41].

density using, $Fp = J_c \times H$, where, J_c is the critical current density and H is the magnetic field. The normalized pinning force density is plotted as a function of reduced magnetic field ($h = H/H_{irr}$) in Fig 12 (a-f) and is analyzed using the model developed by Dew-Hughes [59], which has been widely used in many other studies [33, 57, 60, 61]. The magnetic irreversibility field (H_{irr}) is extracted by considering the magnetic field value where $J_c \leq 50$ A/cm², below which the J_c decreases to the noise level. The scaling of the normalized pinning force curves shows a single peak for each sample under study. However, a close inspection of the scaled curves for different T show a slightly poor scaling for $x = 0.108$, 0.12 and 0.18 samples, with two nearby peaks, as shown with arrows in Fig. 12 (b), (c) and (e). On the other hand samples with $x = 0.092$, 0.15 and 0.065 shows a good scaling with only

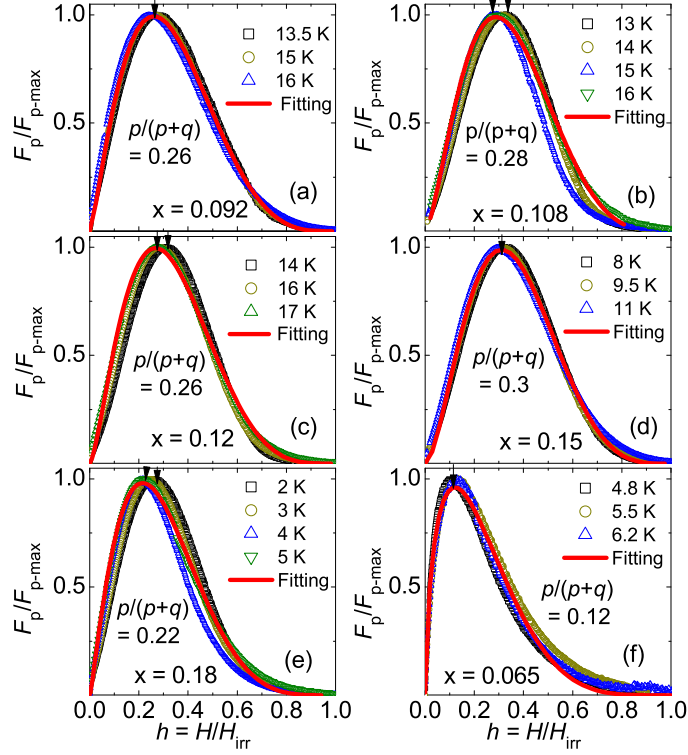


FIG. 12. The normalized pinning force density (F_p/F_{p-max}) as a function of reduced magnetic field, $h = H/H_{irr}$ for for $x =$ (a) 0.092, (b) 0.108, (c) 0.12, (d) 0.15, (e) 0.18, and (f) 0.065 samples. For each sample, data collected at different temperatures scaled to a single curve and the solid line is fit to the scaled curve using, $f_p = A(h)^p(1-h)^q$, where, the parameters p and q defines the pinning characteristics of the sample.

one peak (see Fig. 12 (a), (d) and (f)). A peak behaviour of the scaled curve of pinning force suggests a single dominating pinning behaviour, which may be described in terms of a mathematical expression, $F_p/F_{p-max} = A(h)^p(1-h)^q$, where, A is a multiplicative factor, F_{p-max} is the maximum pinning force density at constant temperature, the parameters p and q provide the details about the pinning mechanism and the peak position is defined by $p/(p+q)$ [60, 62]. This expression was used to fit the scaled pinning force data shown in Fig. 12 (a-f), where, the solid line represents the fitting. The obtained parameters A , p , q and the peak position $p/(p+q)$ for each sample are presented in the table I.

It is known from the Dew-Hughes model that the high value of the peak position ($h > 0.33$) is an indication of dominant δT_c pinning and peak position lower than, $h = 0.33$, suggests the dominant role of δl pinning and point like pinning centers[28, 59, 60, 62].

TABLE I. Parameters obtained by fitting the expression, $F_p/F_{p-max} = A(h)^p(1-h)^q$, to the experimental curves F_p/F_{p-max} vs. h

Samples	A	p	q	$p/(p+q)$
x = 0.092	17.3	1.3	3.6	0.26
x = 0.108	25.4	1.5	3.8	0.28
x = 0.12	24.5	1.4	4.0	0.26
x = 0.15	35.1	1.7	3.9	0.3
x = 0.18	18.2	1.2	4.4	0.22
x = 0.065	6.4	0.6	4.5	0.12

Therefore, the peak positions shown in table I indicates the δl pinning behaviour for almost all investigated samples. However, for $x = 0.065$ (highly underdoped), the peak position is found to be 0.12, which is quite smaller than the overdoped and nearly optimally doped samples. This scenario suggests that the pinning behaviour in overdoped and underdoped regimes are quite different in nature. It is to be noted that the peak position of the scaled pinning force curves is found at $h \sim 0.3$ in the study on a slightly underdoped, $x = 0.09$ sample [58]. In other studies of optimally doped samples ($x = 0.1$), the scaled pinning force curves show $h \geq 0.4$ [29, 57], which would suggest the δT_c pinning. However, Ref. [29] suggests the dominance role of δT_c pinning in the sample, whereas, Ref. [57] claims a strong signature of δl -type pinning. As we know the peak position in the scaled pinning force curves is dependent on the value of irreversibility field, H_{irr} , and based on the criterion to chose the H_{irr} , one may get a smaller or larger value of peak position (h). This shows that a method based on the peak position to describe the pinning mechanism is not robust enough. Therefore, we used the another approach to clear the ambiguity between the δl and δT_c -type pinning in Ni-doped 122 superconductors.

In order to explore the nature of pinning in a series of $\text{BaFe}_{2-x}\text{Ni}_x\text{As}_2$ superconductors, we investigate the temperature dependence of J_c at different magnetic fields and used the model developed by Griessen *et al* [63]. In this model, the pinning due to the spatial variation of the charge carrier mean free path, δl , and the spatial variation of the superconducting transition temperature, δT_c , have been described as, δl ($J_c(t)/J_c(0) = (1-t^2)^{5/2}(1+t^2)^{-1/2}$) and δT_c ($J_c(t)/J_c(0) = (1-t^2)^{7/6}(1+t)^{5/6}$). This model has been widely accepted to

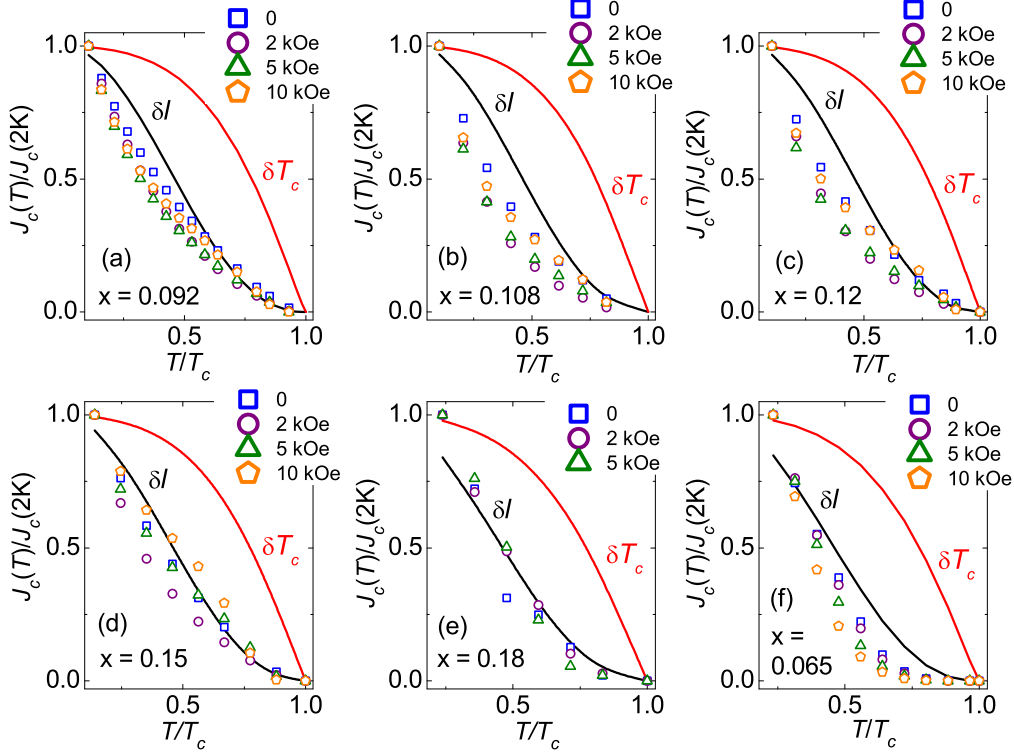


FIG. 13. The normalized critical current density, $J_c(T)/J_c(0)$, as a function of reduced temperature, T/T_c

for $x =$ (a) 0.092, (b) 0.108, (c) 0.12, (d) 0.15, (e) 0.18, and (f) 0.065 samples. The solid lines present the δl and δT_c pinning models. Each sample shows close resemblance with the δl -type pinning mechanism.

investigate the nature of vortex-pinning in superconductors [64, 65]. Figure 13 (a-f), shows $J_c(T)/J_c(2K)$ vs. T/T_c plots at different constant H and suggest the close resemblance with the δl -type pinning mechanism in all six samples under study. This result is consistent with the observation by Shahbazi *et al* [57]. Bitter decoration patterns on optimally doped and overdoped, $\text{BaFe}_{2-x}\text{Ni}_x\text{As}_2$, show a highly inhomogeneous including large and small-scale stripe-like vortex patterns [26] preferably due to the dominant role of δl -type pinning.

IV. SUMMARY AND CONCLUSION

In summary, we studied a series of high quality $\text{BaFe}_{2-x}\text{Ni}_x\text{As}_2$, pnictide superconductors to investigate the doping dependence of the SMP, critical current density and the pinning characteristics. The SMP feature is observed in all samples except in a highly underdoped

one, $x = 0.065$. Interestingly, for $x = 0.092$, the SMP feature is not prominent at low temperatures but is clearly visible above $T = 5$ K. Temperature dependence of the relaxation rate, $R(T)$, suggest a pinning crossover, whereas, its magnetic field dependence, $R(H)$, at different isothermals shows a peak structure. The peak position in $R(H)$, H_{sp} lies in between the characteristic fields H_p and H_{on} associated with the SMP. In reference with other studies, such behaviour is described in terms of vortex-lattice structural phase-transition, which is followed by a pinning crossover. In order to confirm the pinning crossover, magnetic relaxation data was used to extract the activation energy (U) and was analysed using Ma-leys method and collective pinning theory. The analysis unambiguously shows the collective (elastic) to plastic creep crossover as the origin of the SMP in Ni-doped BaFe_2As_2 superconductors. Such pinning crossover may be accompanied with a vortex-lattice structural phase transition below H_p . The critical current density (J_c) estimated using the Bean's critical state model is found to be larger than the threshold limit ($> 10^5$ A/cm²) considered for the technological relevance and even exceeds 1MA/cm² for $x = 0.092$ sample at low temperatures. However, for highly overdoped ($x = 0.18$) and underdoped ($x = 0.065$), the observed J_c is lower than the threshold limit. The pinning behaviour in the samples is analyzed by plotting the normalized pinning force density (F_p/F_{p-max}) as a function of reduced magnetic field ($h = H/H_{irr}$), which suggests the point like pinning centers in the samples. The plot of reduced temperature (T/T_c) dependence of the normalized critical current density ($J_c(T)/J_c(2K)$) suggests that the pinning in the sample is related to the variation of the charge carrier mean free path (δl -type pinning).

ACKNOWLEDGEMENTS

SS acknowledges a post-doctoral fellowship from FAPERJ (Rio de Janeiro, Brazil), processo: E-26/202.848/2016. SSS and LG are supported by CNPq and FAPERJ. LFC is funded by The Leverhulme Trust grant number RPG-2016-306. The work at IOP, CAS is supported by the National Natural Science Foundation of China (11374011 and 11674372), the Strategic Priority Research Program (B) of the Chinese Academy of Sciences (CAS) (XDB07020300 and XDB25000000), and the Youth Innovation Promotion Association of CAS (2016004).

REFERENCES

- [1] Y B Kim, C F Hempstead, and A R Strnad. Critical Persistent Currents in Hard Superconductors. *Phys. Rev. Lett.*, 9:306, 1962.
- [2] P W Anderson. Theory of Flux Creep in Hard Superconductors. *Phys. Rev. Lett.*, 9:309, 1962.
- [3] M R Beasley, R Labusch, and W W Webb. Flux Creep in Type-II Superconductors. *Phys. Rev.*, 181:682, 1969. References therein.
- [4] Y Yeshurun and A P Malozemoff. Giant Flux Creep and Irreversibility in an Y-Ba-Cu-O Crystal: An Alternative to the Superconducting-Glass Model. *Phys. Rev. Lett.*, 60:2202, 1988.
- [5] Y. Abulafia, A. Shaulov, Y. Wolfus, R. Prozorov, L. Burlachkov, Y. Yeshurun, D. Majer, E. Zeldov, H. Wühl, V. B. Geshkenbein, and V. M. Vinokur. Plastic Vortex Creep in $\text{YBa}_2\text{Cu}_3\text{O}_{7-x}$ Crystals. *Phys. Rev. Lett.*, 77:1596, 1996.
- [6] B Rosenstein, B Ya Shapiro, I Shapiro, Y Bruckental, A Shaulov, and Y Yeshurun. Peak Effect and Square-to-Rhombic Vortex Lattice Transition in $\text{La}_{2-x}\text{Sr}_x\text{CuO}_4$. *Phys. Rev. B*, 72:144512, 2005.
- [7] Baruch Rosenstein and Dingping Li. Ginzburg-Landau Theory of Type-II Superconductors in Magnetic Field. *Rev. Mod. Phys.*, 82:109, 2010.
- [8] B Rosenstein and V Zhuravlev. Quantitative Theory of Transport in Vortex Matter of Type-II Superconductors in the Presence of Random Pinning. *Phys. Rev. B*, 76:014507, 2007.
- [9] D Stamopoulos, A Speliotis, and D Niarchos. From the Second Magnetization Peak to Peak Effect. A Study of Superconducting Properties in Nb Films and MgB_2 Bulk Samples. *Supercond. Sci. Technol.*, 17:1261, 2004.
- [10] Y Kamihara, T Watanabe, M Hirano, and H Hosono. Iron-Based Layered Superconductor $\text{La}[\text{O}_{1-x}\text{F}_x]\text{FeAs}$ ($x = 0.05\text{-}0.12$) with $T_c = 26$ K. *J. Am. Chem. Soc.*, 130:3296, 2008.
- [11] Fong-Chi Hsu, Jiu-Yong Luo, Kuo-Wei Yeh, Ta-Kun Chen, Tzu-Wen Huang, Phillip M Wu, Yong-Chi Lee, Yi-Lin Huang, Yan-Yi Chu, Der-Chung Yan, and Maw-Kuen Wu. Superconductivity in the PbO-type Structure $\alpha\text{-FeSe}$. *Proc. National Acad. Sci. USA*, 105:14262, 2008.

- [12] Hai-Hu Wen, Gang Mu, Lei Fang, Huan Yang, and Xiyu Zhu. Superconductivity at 25 K in Hole-Doped $(\text{La}_{1-x}\text{Sr}_x)\text{OFeAs}$. *Europhys. Lett.*, 82:17009, 2008.
- [13] Zhi-An Ren, Jie Yang, Wei Lu, Wei Yi, Xiao-Li Shen, Zheng-Cai Li, Guang-Can Che, Xiao-Li Dong, Li-Ling Sun, Fang Zhou, and Zhong-Xian Zhao. Superconductivity in the Iron-Based F-doped Layered Quaternary Compound $\text{Nd}[\text{O}_{1-x}\text{F}_x]\text{FeAs}$. *Europhys. Lett.*, 82:57002, 2008.
- [14] G R Stewart. Superconductivity in Iron Compounds. *Rev. Mod. Phys.*, 83:1589, 2011.
- [15] C Senatore, R. Flükiger, M Cantoni, G Wu, R H Liu, and X H Chen. Upper Critical Fields Well Above 100 T for the Superconductor $\text{SmFeAsO}_{0.85}\text{F}_{0.15}$ with $T_c = 46$ K. *Phys. Rev. B*, 78:054514, 2008.
- [16] J Jaroszynski, F Hunte, L. Balicas, Youn jung Jo, I Raičević, A Gurevich, D C Larbalestier, F F Balakirev, L Fang, P Cheng, Y Jia, and H H Wen. Upper Critical Fields and Thermally-Activated Transport of $\text{NdFeAsO}_{0.7}\text{F}_{0.3}$ Single Crystal. *Phys. Rev. B*, 78:174523, 2008.
- [17] Zhaosheng Wang, Tao Xie, E Kampert, T Förster, Xingye Lu, Rui Zhang, Dongliang Gong, Shiliang Li, T Herrmannsdörfer, J Wosnitza, and Huiqian Luo. Electron Doping Dependence of the Anisotropic Superconductivity in $\text{BaFe}_{2-x}\text{Ni}_x\text{As}_2$. *Phys. Rev. B*, 92:174509, 2015.
- [18] H Q Yuan, J Singleton, F F Balakirev, S A Baily, G F Chen, J L Luo, , and N L Wang. Nearly Isotropic Superconductivity in $(\text{Ba},\text{K})\text{Fe}_2\text{As}_2$. *Nature (London)*, 457:565, 2009.
- [19] M M Altarawneh, K Collar, C H Mielke, N Ni, S L Budko, and P C Canfield. Determination of Anisotropic H_{c2} up to 60 T in $\text{Ba}_{0.55}\text{K}_{0.45}\text{Fe}_2\text{As}_2$ Single Crystals. *Phys. Rev. B*, 78:220505(R), 2008.
- [20] T Katase, Y Ishimaru, A Tsukamoto, H Hiramatsu, T Kamiya, K Tanabe, and H Hosono. Advantageous Grain Boundaries in Iron Pnictide Superconductors. *Nat. Commun.*, 2:409, 2011.
- [21] J H Durrell, C-B Eom, A Gurevich, E E Hellstrom, C Tarantini, A Yamamoto, and D C Larbalestier. The Behavior of Grain Boundaries in the Fe-based Superconductors. *Rep. Prog. Phys.*, 74:124511, 2011.
- [22] H Hosono, A Yamamoto, H Hiramatsu, and Y Ma. Recent Advances in Iron-based Superconductors Toward Applications. *Materials Today*, 21:278, 2018.
- [23] E V Thuneberg, J Kurkijrvi, and D Rainer. Pinning of a Vortex Line to a Small Defect in Superconductors. *Phys. Rev. Lett.*, 48:1853, 1982.

- [24] R Prozorov, N Ni, M A Tanatar, V G Kogan, R T Gordon, C Martin, E C Blomberg, P Prommapan, J Q Yan, S L Budko, and P C Canfield. Vortex Phase Diagram of $\text{Ba}(\text{Fe}_{0.93}\text{Co}_{0.07})_2\text{As}_2$ Single Crystals. *Phys. Rev. B*, 78:224506, 2008.
- [25] R Kopeliansky, A Shaulov, B Ya Shapiro, Y Yeshurun, B Rosenstein, J J Tu, L J Li, G H Cao, and Z A Xu. Possibility of Vortex Lattice Structural Phase Transition in the Superconducting Pnictide $\text{Ba}(\text{Fe}_{0.925}\text{Co}_{0.075})_2\text{As}_2$. *Phys. Rev. B*, 81:092504, 2010.
- [26] L J Li, T Nishio, Z A Xu, and V V Moshchalkov. Low-field Vortex Patterns in the Multiband $\text{BaFe}_{2-x}\text{Ni}_x\text{As}_2$ Superconductor ($x = 0.1, 0.16$). *Phys. Rev. B*, 83:224522, 2011.
- [27] D Miu, T Noji, T Adachi, Y Koike, and L Miu. On the Nature of the Second Magnetization Peak in $\text{FeSe}_{1-x}\text{Te}_x$ Single Crystals. *Supercond. Sci. Technol.*, 25:115009, 2012.
- [28] K S Pervakov, V A Vlasenko, E P Khlybov, A Zaleski, V M Pudalov, and Yu F Eltsev. Bulk Magnetization and Strong Intrinsic Pinning in Ni-Doped BaFe_2As_2 Single Crystals. *Supercond. Sci. Technol.*, 26:015008, 2013.
- [29] T S Su, Y W Yin, M L Teng, M J Zhang, and X G Li. Angular Dependence of Vortex Dynamics in $\text{BaFe}_{1.9}\text{Ni}_{0.1}\text{As}_2$ Single Crystal. *Materials Research Express*, 1:016003, 2014.
- [30] Shyam Sundar, S Salem-Sugui Jr, H S Amorim, Hai-Hu Wen, K A Yates, L F Cohen, and L Ghivelder. Plastic Pinning Replaces Collective Pinning as the Second Magnetization Peak Disappears in the Pnictide Superconductor $\text{Ba}_{0.75}\text{K}_{0.25}\text{Fe}_2\text{As}_2$. *Phys. Rev. B*, 95:134509, 2017.
- [31] Yong Liu, Lin Zhou, Kewei Sun, Warren E. Straszheim, Makariy A Tanatar, Ruslan Prozorov, and Thomas A Lograsso. Doping Evolution of the Second Magnetization Peak and Magnetic Relaxation in $(\text{Ba}_{1-x}\text{K}_x)\text{Fe}_2\text{As}_2$ Single Crystals. *Phys. Rev. B*, 97:054511, 2018.
- [32] Shyam Sundar, J Mosqueira, A D Alvarenga, D Sora, A S Sefat, and S Salem-Sugui Jr. Study of the Second Magnetization Peak and the Pinning Behaviour in $\text{Ba}(\text{Fe}_{0.935}\text{Co}_{0.065})_2\text{As}_2$ Pnictide Superconductor. *Supercond. Sci. Technol.*, 30:125007, 2017.
- [33] Wei Zhou, Xiangzhuo Xing, Wenjuan Wu, Haijun Zhao, and Zhixiang Shi. Second Magnetization Peak Effect, Vortex Dynamics, and Flux Pinning in 112-Type Superconductor $\text{Ca}_{0.8}\text{La}_{0.2}\text{Fe}_{1-x}\text{Co}_x\text{As}_2$. *Sci. Rep.*, 6:22278, 2016.
- [34] J Hecher, M Zehetmayer, and H W Weber. How the Macroscopic Current Correlates with the Microscopic Flux-line Distribution in a type-II Superconductor: An Experimental Study. *Supercond. Sci. Technol.*, 27:075004, 2014.

- [35] A K Pramanik, L Harnagea, C Nacke, A U B Wolter, S Wurmehl, V Kataev, and B Behner. Fishtail Effect and Vortex Dynamics in LiFeAs Single Crystals. *Phys. Rev. B*, 83:094502, 2011.
- [36] S Salem-Sugui Jr, L Ghivelder, A D Alvarenga, L F Cohen, H Luo, and X Lu. Fishtail and Vortex Dynamics in the Ni-doped Iron Pnictide $\text{BaFe}_{1.82}\text{Ni}_{0.18}\text{As}_2$. *Phys. Rev. B*, 84:052510, 2011.
- [37] S Salem-Sugui Jr, L Ghivelder, A D Alvarenga, L F Cohen, Huiqian Luo, and Xingye Lu. Vortex Dynamics as a Function of Field Orientation in $\text{BaFe}_{1.9}\text{Ni}_{0.1}\text{As}_2$. *Supercond. Sci. Technol.*, 26:025006, 2013.
- [38] D Ahmad, W J Choi, Y I Seo, S-G Jung, Y C Kim, S Salem-Sugui Jr, T Park, , and Y S Kwon. Doping Dependence of the Vortex Dynamics in Single Crystal Superconducting $\text{NaFe}_{1-x}\text{Co}_x\text{As}$. *Supercond. Sci. Technol.*, 30:105006, 2017.
- [39] M. P. Maley, J. O. Willis, H. Lessure, and M. E. McHenry. Dependence of Flux-Creep Activation Energy Upon Current Density in Grain-aligned $\text{YBa}_2\text{Cu}_3\text{O}_{7-x}$. *Phys. Rev. B*, 42:2639(R), 1990.
- [40] M V Feigel'man, V B Geshkenbein, A I Larkin, and V M Vinokur. Theory of Collective Flux Creep. *Phys. Rev. Lett.*, 63:2303, 1989.
- [41] Yanchao Chen, Xingye Lu, Meng Wang, Huiqian Luo, and Shiliang Li. Systematic Growth of $\text{BaFe}_{2-x}\text{Ni}_x\text{As}_2$ Large Crystals. *Supercond. Sci. Technol.*, 24:065004, 2011.
- [42] G. K. Perkins, J. Moore, Y. Bugoslavsky, L. F. Cohen, J. Jun, S. M. Kazakov, J. Karpinski, and A. D. Caplin. Superconducting Critical Fields and Anisotropy of a MgB_2 Single Crystal. *Supercond. Sci. Technol.*, 15:1156, 2002.
- [43] Wei Zhang, Yao-Min Dai, Bing Xu, Run Yang, Jin-Yun Liu, Qiang-Tao Sui, Hui-Qian Luo, Rui Zhang, Xing-Ye Lu, Hao Yang, and Xiang-Gang Qiu. Magnetoresistivity and Filamentary Superconductivity in Nickel-Doped BaFe_2As_2 . *Chin. Phys. B*, 25:047401, 2016.
- [44] M Wang, H Luo, J Zhao, C Zhang, M Wang, K Marty, S Chi, J W Lynn, A Schneidewind, S Li, and P Dai. Electron-Doping Evolution of the Low-Energy Spin Excitations in the Iron Arsenide Superconductor $\text{BaFe}_{2-x}\text{Ni}_x\text{As}_2$. *Phys. Rev. B*, 81:174524, 2010.
- [45] Y Yeshurun, N Bontemps L Burlachkov, and A Kapitulnik. Dynamic Characteristics of the Anomalous Second Peak in the Magnetization Curves of Bi-Sr-Ca-Cu-O. *Phys. Rev. B*, 49:1548, 1994.

- [46] T Tamegai, Y Iye, I Oguro, and K Kishio. Anomalous Peak Effect in Single Crystal $\text{Bi}_2\text{Sr}_2\text{CaCu}_2\text{O}_{8+y}$ Studied by Hall Probe Magnetometry. *Physica C*, 213:33, 1993.
- [47] S P Brown, D Charalambous, E C Jones, E M Forgan, P G Kealey, A Erb, and J Kohlbrecher. Triangular to Square Flux Lattice Phase Transition in $\text{YBa}_2\text{Cu}_3\text{O}_7$. *Phys. Rev. Lett.*, 92:067004, 2004.
- [48] Toshihiro Taen, Yasuyuki Nakajima, Tsuyoshi Tamegai, and Hisashi Kitamura. Enhancement of Critical Current Density and Vortex Activation Energy in Proton-Irradiated Co-Doped BaFe_2As_2 . *Phys. Rev. B*, 86:094527, 2012.
- [49] R Griessen, A F Th Hoekstra, H H Wen, G Doombos, and H G Schnack. Negative- μ Vortex Dynamics in High- T_c Superconducting Films. *Physica C: Superconductivity and Its Applications*, 282-287:347, 1997.
- [50] S Salem-Sugui Jr, L Ghivelder, A D Alvarenga, L F Cohen, K A Yates, K Morrison, J L Pimentel Jr, Huiqian Luo, Zhaosheng Wang, and Hai-Hu Wen. Flux Dynamics Associated with the Second Magnetization Peak in the Iron Pnictide $\text{Ba}_{1-x}\text{K}_x\text{Fe}_2\text{As}_2$. *Phys. Rev. B*, 82:054513, 2010.
- [51] Yue Sun, Toshihiro Taen, Yuji Tsuchiya, Sunseng Pyon, Zhixiang Shi, and Tsuyoshi Tamegai. Magnetic Relaxation and Collective Vortex Creep in $\text{FeTe}_{0.6}\text{Se}_{0.4}$ Single Crystal. *Europhys. Lett.*, 103:57013, 2013.
- [52] N Haberkorn, M Miura, B Maiorov, G F Chen, W Yu, and L Civale. Strong Pinning and Elastic to Plastic Vortex Crossover in Na-doped CaFe_2As_2 Single Crystals. *Phys. Rev. B*, 84:094522, 2011.
- [53] M. E. McHenry, S. Simizu, H. Lessure, M. P. Maley, J. Y. Coulter, I. Tanaka, and H. Kojima. Dependence of the Flux-creep Activation Energy on the Magnetization Current for a $\text{La}_{1.86}\text{Sr}_{0.14}\text{CuO}_4$ Single Crystal. *Phys. Rev. B*, 44:7614, 1991.
- [54] Charles P Bean. Magnetization of High-Field Superconductors. *Rev. Mod. Phys.*, 36:31, 1964.
- [55] Dongjoon Song, Shigeyuki Ishida, Akira Iyo, Masamichi Nakajima, Jun ichi Shimoyama, Michael Eisterer, and Hiroshi Eisaki. Distinct Doping Dependence of Critical Temperature and Critical Current Density in $\text{Ba}_{1-x}\text{K}_x\text{Fe}_2\text{As}_2$ Superconductor. *Sci. Rep.*, 6:26671, 2016.
- [56] Ilaria Pallegchi, Michael Eisterer, Andrea Malagoli, and Marina Putti. Application Potential of Fe-Based Superconductors. *Supercond. Sci. Technol.*, 28:114005, 2015.

- [57] M Shahbazi, X L Wang, K Y Choi, and S X Dou. Flux Pinning Mechanism in $\text{BaFe}_{1.9}\text{Ni}_{0.1}\text{As}_2$ Single Crystals: Evidence for Fluctuation in Mean Free Path Induced Pinning. *Applied Physics Letters*, 103:032605, 2013.
- [58] D L Sun, Y Liu, and C T Lin. Comparative Study of Upper Critical Field H_{c2} and Second Magnetization Peak H_{sp} in Hole and Electron-Doped BaFe_2As_2 Superconductor. *Phys. Rev. B*, 80:144515, 2009.
- [59] D Dew-Hughes. Flux Pinning Mechanisms in Type-II Superconductors. *Philosophical Magazine*, 30:293, 1974.
- [60] M R Koblishka, A J J van Dalen, T Higuchi, S I Yoo, and M Murakami. Analysis of Pinning in $\text{NdBa}_2\text{Cu}_3\text{O}_{7-\delta}$ Superconductors. *Phys. Rev. B*, 58:2863, 1998.
- [61] Md Matin, L S Sharath Chandra, M K Chattopadhyay, R K Meena, Rakesh Kaul, M N Singh, A K Sinha, and S B Roy. Magnetic Irreversibility and Pinning Force Density in the Ti-V Alloys. *Journal of Applied Physics*, 113:163903, 2013.
- [62] Michael R Koblishka and Miryala Muralidhar. Pinning Force Scaling Analysis of Fe-based High- T_c Superconductors. *International Journal of Modern Physics B*, 30:1630017, 2016.
- [63] R Griessen, Hai-Hu Wen, A J J van Dalen, B Dam, J Rector, and H G Schnack. Evidence for Mean Free Path Fluctuation Induced Pinning in $\text{YBa}_2\text{Cu}_3\text{O}_7$ and $\text{YBa}_2\text{Cu}_4\text{O}_8$ Films. *Phys. Rev. Lett.*, 72:1910, 1994.
- [64] V A Vlasenko, K S Pervakov, S Yu Gavrilkin, and Yu F Eltsev. Unconventional Pinning in Iron Based Superconductors of 122 Family. *Physics Procedia*, 67:952–957, 2015.
- [65] S R Ghorbani, Xiao-Lin Wang, M S A Hossain, Q W Yao, S X Dou, Sung-IK Lee, K C Chung, and Y K Kim. Strong Competition Between the δl and δT_c Flux Pinning Mechanisms in MgB_2 Doped with Carbon Containing Compounds. *Journal of Applied Physics*, 107:113921, 2010.